Biomaterials Science

ROYAL SOCIETY OF CHEMISTRY

PAPER

View Article Online
View Journal | View Issue

Cite this: *Biomater. Sci.*, 2025, **13**, 4232

Antimicrobial cobaltocenium copolymers: tuning amphiphilicity against NDM-1 bacteria†

Md Waliullah Hossain,[a] Ian Brand,[a] Swagatam Barman,[a] Alimi Abidoun,[a] JiHyeon Hwang,[a] Adam Parris,[a] Xiaoming Yang,[b] Prakash Nagarkatti,[b] Mitzi Nagarkatti[b] and Chuanbing Tang *[a]

The emergence of Gram-negative superbugs coupled with a steep decline in antibiotic pipelines has imposed a serious threat to global public health. Cationic metallopolymers have gained significant attention due to their antimicrobial efficacy. In this work, we developed a range of broad-spectrum antimicrobial cobaltocenium and ammonium containing copolymers with different compositions, which attain the amphiphilic balance without compromising the total charges for enhanced interaction with bacterial membranes. The copolymers showed high antimicrobial efficacy with greater selectivity than the corresponding ammonium-containing methacrylate polymers. The mechanistic investigations of the lead polymer using bacterial strains harboring the New Delhi metallo-β-lactamase (NDM-1) enzyme revealed its membrane-active nature. The copolymer with 69% dimethyl cobaltocenium showed a minimal increase in the minimal inhibitory concentration over 14 passages, whereas polymyxin-B showed a 256-fold increase. These findings provided insights into metallopolymers with optimal amphiphilicity as potent antimicrobial agents to tackle Gram-negative superbugs.

Received 1st April 2025,
Accepted 8th June 2025

DOI: 10.1039/d5bm00497g

rsc.li/biomaterials-science

1. Introduction

Antimicrobial resistance (AMR) is no longer a future predicament but one of the greatest challenges to public health worldwide.[1,2] Antibiotics are arguably among the greatest discoveries ever for treating bacterial infections.[3] However, there is a significant reduction in new antibiotic discovery compared to the growing antibiotic resistance. Between 1962 and 2000, there were no reports of discovering a new class of antibiotics that can treat common and deadly infections associated with Gram-negative bacteria.[4] Bacterial resistance to antibiotics arises through various mechanisms.[5,6] Gram-positive bacteria possess a thick, net negatively-charged peptidoglycan layer, while Gram-negative bacteria have an asymmetric lipid bilayer, which contains a significant amount of negatively-charged lipopolysaccharides (LPS).[7] Many of the latter, listed in the World Health Organization's 'critical group' of priority pathogens, present a greater threat due to the emergence of extended-spectrum serine β-lactamase (ESBL) and New Delhi metallo-β-lactamase (NDM) containing strains.[8] In particular, treatment options for NDM-1-producing bacteria remain scarce.[9,10] To bypass these resistance mechanisms, developing antimicrobial agents that leverage amphiphilicity to disrupt bacterial membranes offers a promising universal strategy.[11]

Antimicrobial peptides (AMPs) are part of the innate immune system of multicellular eukaryotes that can prevent infectious diseases by combating pathogenic bacteria, viruses, and fungi.[12] AMPs are composed of varying combinations of cationic, hydrophilic, and hydrophobic groups, possessing overall positive charges, which allow them to selectively target negatively charged bacterial membranes.[13–17] Their membrane-disrupting properties make them effective against multidrug-resistant (MDR) bacteria.[18,19] However, clinical use is limited due to low bioavailability, poor stability and high manufacturing cost. Synthetic polymers mimicking AMPs offer a scalable, cost-effective alternative, retaining cationic charges and amphiphilicity for antibacterial activity.[20–24] Ongoing research aims to optimize these AMP-mimicking polymers for enhanced efficacy and broader clinical application.[25–34]

Metallopolymers have emerged as a unique class of polymers, which combine an organic polymeric framework with functional inorganic metal centers to synergistically tune the properties of the combined framework.[35–38] Although the broad impacts of this emerging class of polymers remain underexplored in the field of antimicrobial therapeutics,[39–44] cobaltocenium-containing homopolymers have been reported to form bioconjugates with antibiotics and used as adjuvants

[a]Department of Chemistry and Biochemistry, University of South Carolina, Columbia, SC 29208, USA. E-mail: tang4@mailbox.sc.edu
[b]Department of Pathology, Microbiology and Immunology, University of South Carolina, School of Medicine, Columbia, SC 29209, USA

† Electronic supplementary information (ESI) available. See DOI: https://doi.org/10.1039/d5bm00497g

to resensitize antibiotics.[44–47] However, most of these polymers alone exhibit poor antimicrobial activity. While adjuvants help revive antibiotics, developing new antimicrobial agents is crucial for preventing resistance and strengthening the therapeutic arsenal. Ammonium-containing polymers have been studied extensively as antimicrobial agents,[48,49] employing binary and ternary systems to generate libraries of copolymers with various compositions to achieve significant efficacy.[50,51]

Herein, we report cobaltocenium-containing methacrylate copolymers as novel antimicrobial agents that combine with primary ammonium charges to tune the amphiphilicity without altering the overall charge of the polymers. In addition, cobaltocenium and dimethyl substituted cobaltocenium were compared to elucidate their effect on antimicrobial efficacy. The introduction of the latter moiety is considered as an additional handle to alter the hydrophobicity of the cobaltocenium moieties. The antimicrobial activity of these copolymers was tested against methicillin-resistant *S. aureus* (MRSA) strains and Gram-negative bacteria, including NDM-1 strains, and their structure–activity relationship was evaluated. Killing kinetics was performed against both planktonic and stationary bacterial cells harboring NDM-1. Mechanistic investigations, including outer membrane permeability, membrane depolarization, LPS inhibition assay, and alteration of bacterial surface potential, revealed membrane-perturbing properties of these cobaltocenium-containing copolymers. Furthermore, the resistance profile of a lead copolymer was assessed for 14 passages.

2. Results

2.1. Synthesis of cobaltocenium-containing copolymers

Cobaltocenium is a unique metallocene cation, which has previously shown electrostatic interaction with anions,[52,53] anionic polyelectrolytes,[54,55] and negatively charged bacterial membranes.[45,46] The balance of cationic charges and amphiphilicity plays a crucial role in designing an effective antimicrobial polymer.[2] To tune amphiphilicity, cobaltocenium was quantitatively incorporated into methacrylate copolymers, as shown in Scheme 1. A homopolymer (**PAEMA**) of 2-aminoethyl methacrylate with a molecular weight of 4.0 kDa was first synthesized *via* Reversible Addition Fragmentation Transfer (RAFT) polymerization using 2-cyano-2-propyl benzodithioate (CPB) as a chain transfer agent, and 2,2′-azobisisobutyronitrile (AIBN) as an initiator (Scheme S1†), according to a previously reported literature study.[56] Cobaltocenium carboxylic acid and dimethyl substituted cobaltocenium carboxylic acid were synthesized according to prior work.[57] Attachment of cobaltocenium to **PAEMA** was achieved using an amide coupling reaction. Successful integration of cobaltocenium was indicated by the presence of aromatic cyclopentadienyl (Cp) protons at 6.1–6.4 ppm and 5.7–6.0 ppm from ^{1}H NMR (Fig. 1). For dimethyl substituted cobaltocenium, the Cp proton peaks appear at 5.5–6.2 ppm and the two methyl peaks appear approximately at 2.0–2.2 ppm and 2.3–2.5 ppm (Fig. 1). By tuning the compositions, we could control the percentages of cobaltocenium (CC) and dimethyl cobaltocenium (dmCC) and obtain six different random copolymers (Table 1). Finally, ion exchange was performed to change the counter ion from PF_6^- to Cl^- for much enhanced solubility in the culture media and to prevent aggregation in aqueous media.[58] All polymers were water soluble and were tested up to 20 mg mL^{-1}. Polymer size and zeta potential were determined at different concentrations (0.5, 1, and 2 mg mL^{-1}) using dynamic light scattering (DLS) (see ESI Table S1†).[59] At these concentrations, the homopolymer P1 did not show any aggregation. However, CC-substituted copolymers (P2–P4) observed the hydrodynamic diameter D_H ranging from 6.9 nm to 22.4 nm, while dmCC-substituted copolymers showed a range of 40.9–70.9 nm. This indicated that the more hydrophobic dmCC likely induced the aggregation of copolymers. Zeta potential analysis revealed that the homopolymer P1 has the lowest zeta potential of <10 mV possibly due to the absence of aggregation, whereas the CC-substituted copolymers increased in the zeta potential ranging from ~+14 mV to ~+25 mV and dmCC-substituted copolymers showed an even higher zeta potential ranging from ~+29 mV to ~+47 mV.

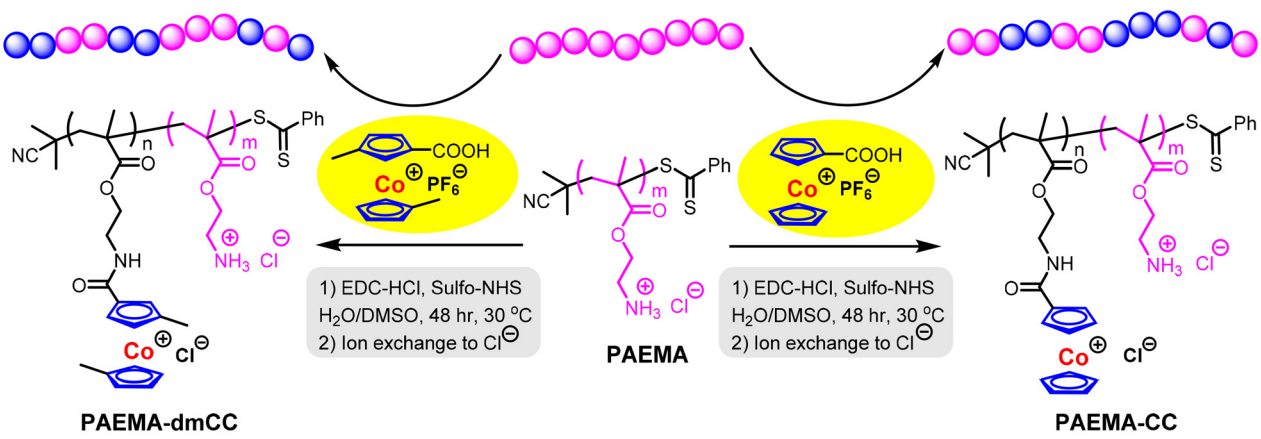

Scheme 1 Synthesis of random copolymers of cobaltocenium (CC) or dimethyl substituted cobaltocenium (dmCC) with 2-aminoethyl methacrylate *via* post modification with poly(2-aminoethyl methacrylate) (**PAEMA**) that was prepared *via* RAFT polymerization.

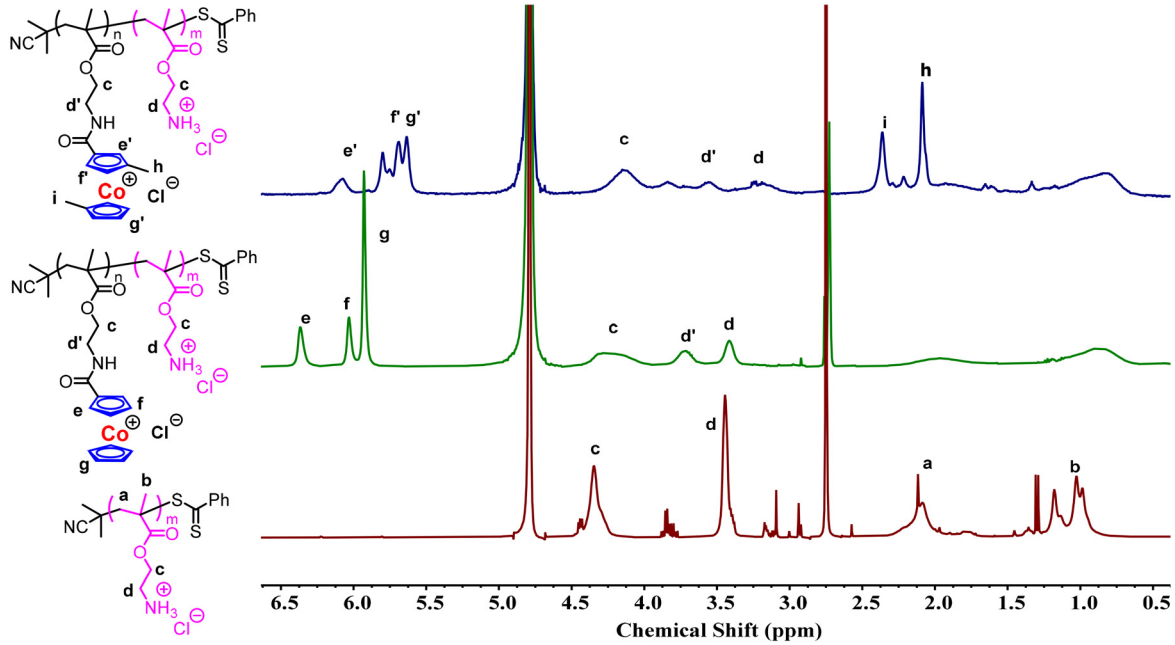

Fig. 1 ^{1}H NMR spectra of the **PAEMA** homopolymer (P1), the cobaltocenium containing copolymer (P2) and the dimethyl substituted cobaltocenium containing copolymer (P5) (deuterated solvent: D_2O).

Table 1 Compositions of copolymers with molar percentages of charge moieties based on ^{1}H NMR analysis

Polymer	Ammonium (mol%)	Cobaltocenium (mol%)	Dimethyl cobaltocenium (mol%)	Molecular weight[a] (kDa)
P1	100	0	0	4.0
P2	58	42	0	6.1
P3	50	50	0	6.5
P4	19	81	0	8.1
P5	46	0	54	7.1
P6	42	0	58	7.3
P7	31	0	69	7.9

[a] Estimated molecular weight from the end-group analysis of ^{1}H NMR.

2.2. Antimicrobial activity of cobaltocenium-containing copolymers

The antimicrobial activity of CC- or dmCC-containing copolymers (P2–P7) was determined against two strains of Gram-positive methicillin-resistant *S. aureus* (MRSA) and three Gram-negative bacterial strains: *E. coli*, *P. aeruginosa*, and *E. cloacae*. It was carried out through a broth microdilution method following a well-established protocol adopted by the Clinical Laboratory Standards Institute (CLSI) and described as the minimum inhibitory concentration (MIC).[60] Polymers were tested at concentrations ranging from 256 μg mL^{-1} to 0.5 μg mL^{-1}. The results are included in Table 2.

While P1 showed no activity against Gram-negative bacteria, it was moderately active against both MRSA strains with a MIC_{90} value of 32 μg mL^{-1}. For cobaltocenium copolymers, we noticed that with an increasing percentage of cobaltocenium, the copolymers exhibited higher efficacy against Gram-negative strains. The dmCC-containing copolymers showed higher activity compared to their unsubstituted counterparts. To further investigate the effect of cobaltocenium, we tested the copolymers against MDR Gram-negative strains including NDM-1 bearing strains, as shown in Table 3. We found a more prominent effect of dmCC in these strains where copolymers with moderate (P5: **PAEMA-dmCC**54%, P6: **PAEMA-dmCC**58%) to higher (P7: **PAEMA-dmCC**69%) fractions exhibited very high activities with MIC_{90} values as low as 2 μg mL^{-1}, whereas CC-containing copolymers showed a gradual enhancement in activities from lower (P2: **PAEMA-CC**42%, P3: **PAEMA-CC**50%) to higher fractions (P4: **PAEMA-CC**80%), reaching a MIC_{90} value of 4 μg mL^{-1}.

2.3 Bactericidal kinetics against planktonic and stationary bacteria

Carbapenem-resistant Enterobacteriaceae (CRE) are among the urgent threat pathogens. These bacteria can render antibiotics ineffective by producing NDM-1 enzyme to hydrolyze β-lactam antibiotics.[6] Thus, we intended to perform killing kinetics of cobaltocenium copolymers against two NDM-1 containing

Table 2 Minimum inhibitory concentrations of **PAEMA** (P1) and CC- or dmCC-containing copolymers (P2–P7) against Gram-negative strains, *Escherichia coli* (ATCC-11775), *Pseudomonas aeruginosa* (ATCC-10145), and *Enterobacter cloacae* (ATCC-13047), and two Gram-positive strains, MRSA-1 (BAA-1717) and MRSA-2 (BAA-44) (MIC_{90} values are reported in μg mL^{-1})

Bacterial strain	P1	P2 (CC42%)	P3 (CC50%)	P4 (CC81%)	P5 (dmCC54%)	P6 (dmCC58%)	P7 (dmCC69%)
E. coli	256	128	128	32	32	16	16
P. aeruginosa	256	128	128	128	64	32	32
E. cloacae	256	256	128	4	64	16	8
MRSA-1	32	16	16	4	4	16	2
MRSA-2	32	16	8	2	4	16	4

Table 3 Minimum inhibitory concentrations of **PAEMA** (P1) and cobaltocenium-containing copolymers (P2–P7) against MDR Gram-negative strains, MDR *E. coli*-1 (BAA-2452) (NDM-1^+), MDR *E. coli*-2 (BAA-2471) (NDM-1^+), MDR *E. hormaechei* (BAA-2468) (NDM-1^+), MDR *K. pneumoniae* (BAA-2473) (NDM-1^+), and MDR *P. aeruginosa* (BAA-2108) (MIC_{90} values are reported in μg mL^{-1})

Bacterial strains	P1	P2 (CC42%)	P3 (CC50%)	P4 (CC81%)	P5 (dmCC54%)	P6 (dmCC58%)	P7 (dmCC69%)
E. coli-1	128	32	16	4	8	4	4
E. coli-2	>256	64	32	4	16	8	8
E. hormaechei	256	128	32	4	4	32	4
K. pneumoniae	>256	128	32	4	16	2	4
P. aeruginosa	64	64	32	8	8	32	2

Gram-negative strains: MDR *E. coli* (BAA-2471), MDR *K. pneumoniae* (BAA-2473). Based on the growth conditions, bacteria can multiply in different sub-populations: planktonic and stationary phases. Planktonic bacterial cells grow under favorable conditions, while, in contrast, stationary bacterial cells grow under nutrient-starved conditions. Antibiotics that can inhibit planktonic bacteria (metabolically active) often fail in treating stationary bacteria (metabolically inactive) because of the difference in cellular metabolic processes.[2]

First, we treated planktonic bacterial cells of both strains and observed that it took 8 hours for the copolymers (P4, P6, and P7) to kill the bacteria completely. During treatment against MDR *E. coli*, all copolymers at different concentrations (2×, 4×, and 8× MIC_{90}) showed a significant reduction of bacteria within 4 hours (~4 log reduction) (Fig. 2A). For MDR *K. pneumoniae*, an even faster reduction of bacterial colonies was noticed. Within 2 hours, P6 achieved ~2.5 log reduction, whereas P4 and P7 achieved ~4 log reduction, indicating more efficient inhibition of bacteria with higher cobaltocenium contents in the copolymers (Fig. 2B).

The better performing copolymers P4 and P7 were selected to treat stationary phase bacteria. Two β-lactam antibiotics, Aztreonam and Imipenem, were used as antibiotic controls at concentrations not lower than the copolymers. At 2 hours, the control (without any treatment) and antibiotics did not induce reduction, while all concentrations (4× and 8× MIC_{90}) of the copolymers displayed significant reduction. P7 was able to eliminate MDR *E. coli* completely within 4 hours, whereas the antibiotics displayed only ~2 log reduction up to 12 hours (Fig. 2C). Against MDR *K. pneumoniae*, similar results were observed for copolymer P7 and antibiotic treatment (Fig. 2D). These outcomes indicated significant killing efficiency of the copolymers against both planktonic and stationary cells of Gram-negative bacteria.

2.4. Toxicity and selectivity

It is crucial to evaluate the biocompatibility of antimicrobial polymers. Hemolysis of mouse red blood cells (RBCs) was assessed and is summarized in Fig. 2E. All polymers exhibited a low hemolysis rate at various concentrations, and the HC_{50} (concentration of the test drug required for 50% lysis of RBCs) was found to be >1000 μg mL^{-1}. It is noteworthy that dmCC-containing copolymers (P5, P6, and P7) showed lower hemolysis than the precursor polymer (P1).

The therapeutic index is an indicator of the applicability of a new antimicrobial agent. A suitable antimicrobial agent should display selective antimicrobial characteristics towards pathogenic microbes over mammalian cells. The selectivity of polymers is defined as the ratio between the concentrations leading to 50% hemolysis (HC_{50}) and the minimum inhibitory concentration (MIC_{90}) of polymer required to inhibit bacterial growth (selectivity = HC_{50}/MIC_{90}). Higher selectivity indicates selective killing of pathogens over mammalian cells. Since all polymers have HC_{50} over 1000 μg mL^{-1}, the selectivity index depends on the MICs of the polymers. Table 4 shows the selectivity index of the copolymers (P3–P7) against Gram-negative bacterial strains, excluding precursor homopolymer P1 and copolymer P2 (**PAEMA-CC**42%) as they have high MIC values against bacterial strains. A higher selectivity was obtained for copolymers with higher cobaltocenium contents. The selectivity index is in the range of >31 to >500, which manifests excellent selectivity toward bacterial cells over mammalian cells.

2.5. Mechanisms of action

2.5.1 Permeability of the outer membrane. Cationic AMPs are believed to kill bacteria by disrupting membranes through a combination of electrostatic and hydrophobic interactions.[24]

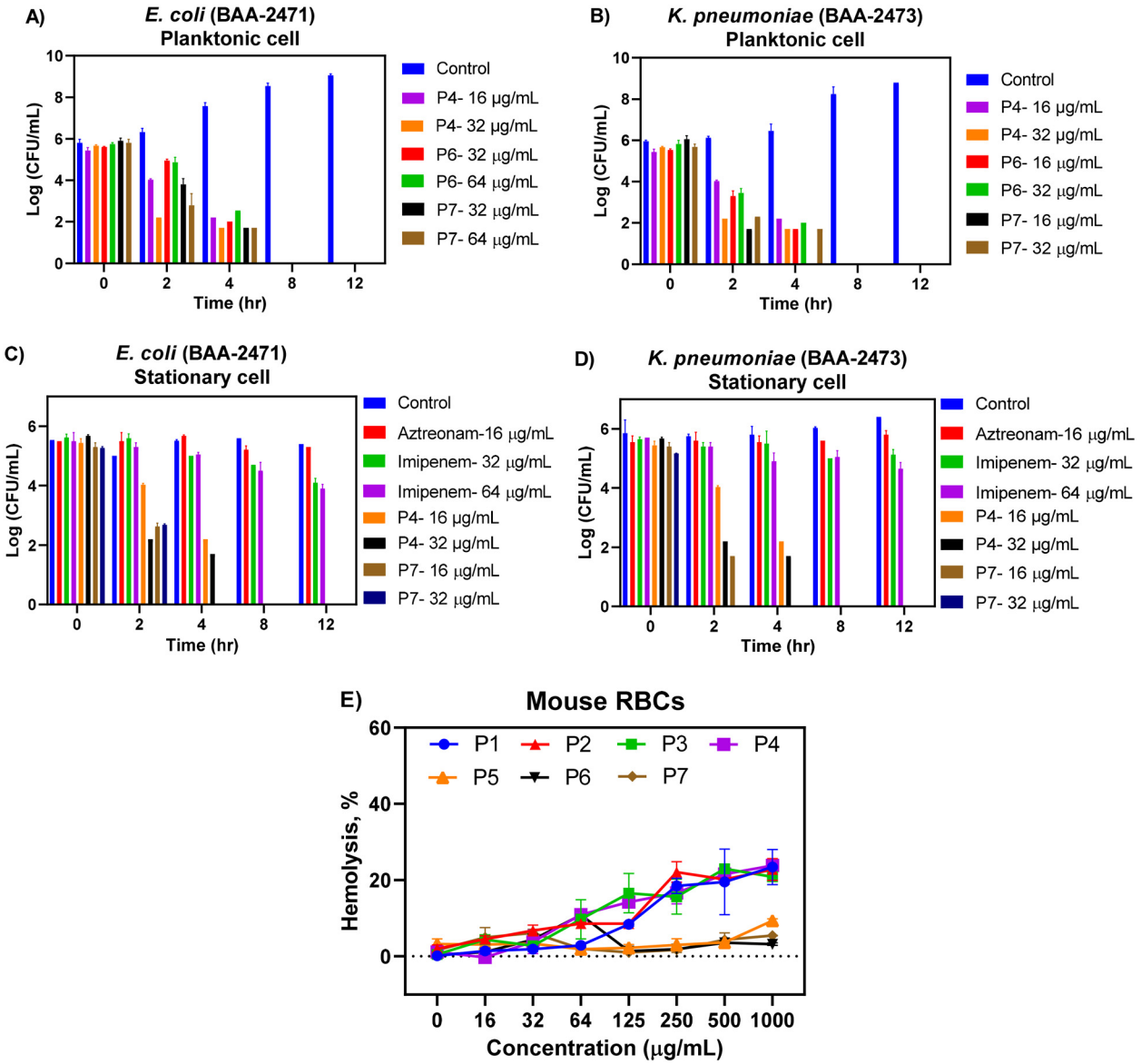

Fig. 2 Time-kill kinetics of MDR Gram-negative strains, *E. coli* (BAA-2471) and *K. pneumoniae* (BAA-2473): (A and B) planktonic bacteria using P4, P6, and P7 copolymers; (C and D) stationary bacteria using P4, P7 and antibiotics (Aztreonam and Imipenem); and (E) hemolysis of mouse red blood cells (RBCs) using polymers.

Table 4 Selectivity index of active CC and dmCC-containing copolymers (P3–P7) against MDR Gram-negative strains: MDR *E. coli*-1 (BAA-2452) (NDM-1$^+$), MDR *E. coli*-2 (BAA-2471) (NDM-1$^+$), MDR *E. hormaechei* (BAA-2468) (NDM-1$^+$), MDR *K. pneumoniae* (BAA-2473) (NDM-1$^+$), and MDR *P. aeruginosa* (BAA-2108)

Bacterial strains	P3 (CC50%)	P4 (CC81%)	P5 (dmCC54%)	P6 (dmCC58%)	P7 (dmCC69%)
E. coli-1	>62.5	>250	>125	>250	>250
E. coli-2	>31.25	>250	>62.5	>125	>125
E. hormaechei	>31.25	>250	>250	>31.25	>250
K. pneumoniae	>31.25	>250	>62.5	>500	>250
P. aeruginosa	>31.25	>125	>125	>31.25	>500

Thus, these cobaltocenium copolymers were assessed for their ability to compromise membranes. Gram-negative bacteria are intrinsically resistant to different antibiotics due to the presence of an outer membrane, which consists of an asymmetric bilayer of lipopolysaccharides (LPSs) and phospholipids with different transport proteins that can down-regulate the uptake of antibiotics.[61] The outer membrane being inherently more rigid than the inner membrane can slow down the diffusion of

hydrophobic drugs, and narrow pore channels can limit the intake of hydrophilic drugs.[7] Thus, disruption of the outer membrane can be utilized as an effective strategy to combat Gram-negative bacteria. P7 was chosen as the lead copolymer to investigate the mechanistic insights using a 1-*N*-phenylnaphthylamine (NPN) dye assay against MDR *E. coli* (BAA-2471) and MDR *K. pneumoniae* (BAA-2473). Hydrophobic NPN shows diminished fluorescence in an aqueous environment but interacts strongly with phospholipids and fluoresces if the outer membrane is permeabilized.[17]

Both planktonic and stationary bacterial cells were treated separately with P7 at different concentrations (1×, 2×, and 4× MIC_{90}). In the case of MDR *E. coli*, increased fluorescence was observed with higher doses of the copolymer, indicating dose-dependent damage to the outer membrane of planktonic bacteria (Fig. 3A). For stationary bacteria, the fluorescence intensity also increased but was not as prominent as planktonic bacteria, indicating acquired resistance by the bacteria though not enough to prevent membrane rupture (Fig. 3C). Similar observations were found against MDR *K. pneumoniae*, where lower doses of the polymer caused less damage to the outer membrane and higher doses showed enhanced perturbation for both planktonic and stationary bacteria (Fig. 3B and D).

2.5.2 Bacterial membrane depolarization. The movement of protons in bacteria is dependent on the electrical potential and transmembrane proton gradient, which are combinedly known as the proton motive force (PMF).[62] A charged polymer can disrupt the bacterial membrane and imbalance the PMF to eliminate bacteria. To probe this, a membrane potential sensitive dye 3,3′-dipropylthiadicarbocyanine iodide ($DiSC_3$) was used. Under normal conditions, this dye accumulates on the bacterial membrane and quenches its fluorescence. But if the membrane is disturbed, the dye leaks out and shows increased fluorescence.[44] Up to 20% increase in fluorescence was observed for the lead polymer P7, at 8× MIC_{90} against MDR *E. coli* (Fig. 3E), whereas about 120% increase in fluorescence was noticed under the same conditions for MDR *K. pneumoniae* (Fig. 3F). Altogether, moderate to high membrane depolarization can be caused by the polymer.

2.5.3 Lipopolysaccharide (LPS) inhibition assay. The activity of AMP-mimicking polymers against Gram-negative bacteria can be further explained by their interaction with LPS molecules, one of the major components in the outer membrane of Gram-negative bacteria. The lead polymer P7 was used to perform an MIC assay against two Gram-negative MDR bacteria in the presence of different concentrations of LPS. In both bacteria, after adding 50 μg mL^{-1} LPS the MIC value increased by 8-fold (Fig. 4A and B) (MIC_{90} values: 8 μg mL^{-1} against MDR *E. coli* and 4 μg mL^{-1} against MDR *K. pneumoniae*). This experiment indicated that the cationic polymer has high electrostatic interactions with the negatively charged LPS molecules added externally, and hence the increase in MIC values. Therefore, the polymers can bind strongly to the Gram-negative bacterial membrane, causing irreversible damage and eventual cell death.

2.5.4 Bacterial surface charge alteration. As mentioned previously, bacterial membranes are negatively charged. The electrostatic interaction between the cationic polymer and the anionic membrane can be verified by zeta-potential measurements. In the case of MDR *E. coli*, the initial zeta potential was −21 mV, as the polymer dosage was increased the potential shifted towards positive reaching +1.3 mV with 256 μg mL^{-1} P7 (Fig. 4C). For MDR *K. pneumoniae*, a more prominent change was observed with the zeta potential shifting from −28 mV to +18.7 mV for 256 μg mL^{-1} P7 (Fig. 4D). These findings again reinforced that the polymer was able to destabilize its surface potential, thus effectively disrupting the bacterial cell envelope.

2.6. Propensity to resistance

One major cause of drug resistance in antibiotics is sub-lethal and/or repeated dosing of antibiotics, which can lead to the formation of multidrug resistant mutant strains. AMP-mimicking polymers usually have an advantage over conventional small molecular antibiotics due to their membrane targeting properties. To investigate the propensity to resistance, NDM-1 containing MDR *K. pneumoniae* was treated with the lead polymer P7 and polymyxin-B. The bacteria were exposed to 14 serial passages. The polymer exhibited only a 2-fold increase in the MIC by passage 11, in contrast to polymyxin B, which showed a 256-fold MIC increase by passage 7 and maintained at that level throughout the remainder of the treatment period (Fig. 4E). The experiment suggested that the polymer exhibited a markedly low propensity for resistance development compared to conventional antibiotics, likely due to its membrane-targeting mechanism.

3. Discussion

Gram-negative bacteria, especially NDM-1 producing strains, are of urgent concern with no efficient treatment strategy currently in existence. Therefore, new antimicrobial agent discovery besides conventional antibiotics can work as a standalone or combined synergistic treatment method. In this work, we aim to combat Gram-negative bacteria by developing a library of metallopolymers with two charged species to unveil a new approach towards AMP-mimicking polymers. Combining cobaltocenium with the primary ammonium containing methacrylate polymer and carefully controlling the incorporation of a cobaltocenium moiety, an effective amphiphilic balance was obtained without compromising the overall cationic nature of the polymer. In particular, copolymers P4 (CC81%) and P7 (dmCC69%) with a higher percentage of cobaltocenium stood out with excellent antimicrobial activity against Gram-negative bacteria compared to the rest of the polymers. The bactericidal kinetics revealed complete eradication of MDR bacterial strains (*E. coli* and *K. pneumoniae*) within a short time with the copolymer treatment, reflecting the fast-acting properties of AMP mimicking agents. Another significant feature of antimicrobial agents is their high selectivity towards bacterial cells. The copolymers showed hemocompatibility up to

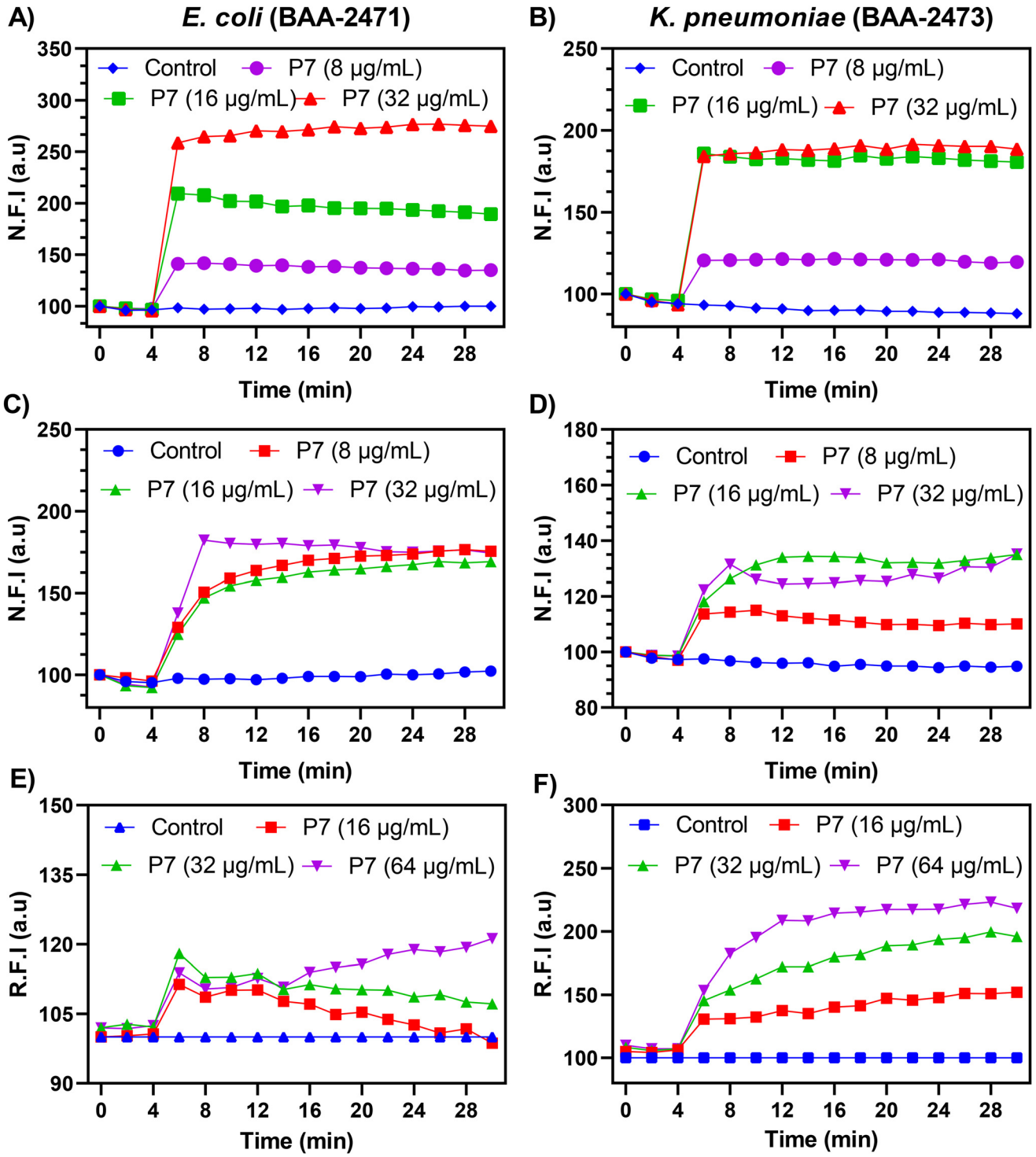

Fig. 3 Outer membrane permeabilization of planktonic cells: (A) MDR *E. coli* (BAA-2471) and (B) MDR *K. pneumoniae* (BAA-2473); outer membrane permeabilization of stationary cells: (C) MDR *E. coli* (BAA-2471) and (D) MDR *K. pneumoniae* (BAA-2473); bacterial membrane depolarization: (E) MDR *E. coli* (BAA-2471) and (F) MDR *K. pneumoniae* (BAA-2473).

>1000 μg mL^{-1} and were highly selective towards Gram-negative bacterial cells.

Furthermore, we performed an in-depth analysis of the mechanistic action of the most active copolymer P7, with an emphasis on NDM-1 containing bacteria. The outer membrane and proton motive force (PMF) of Gram-negative bacteria make multiple treatments fail, thus resulting in MDR bacteria. The copolymer was able to disrupt the outer membrane and

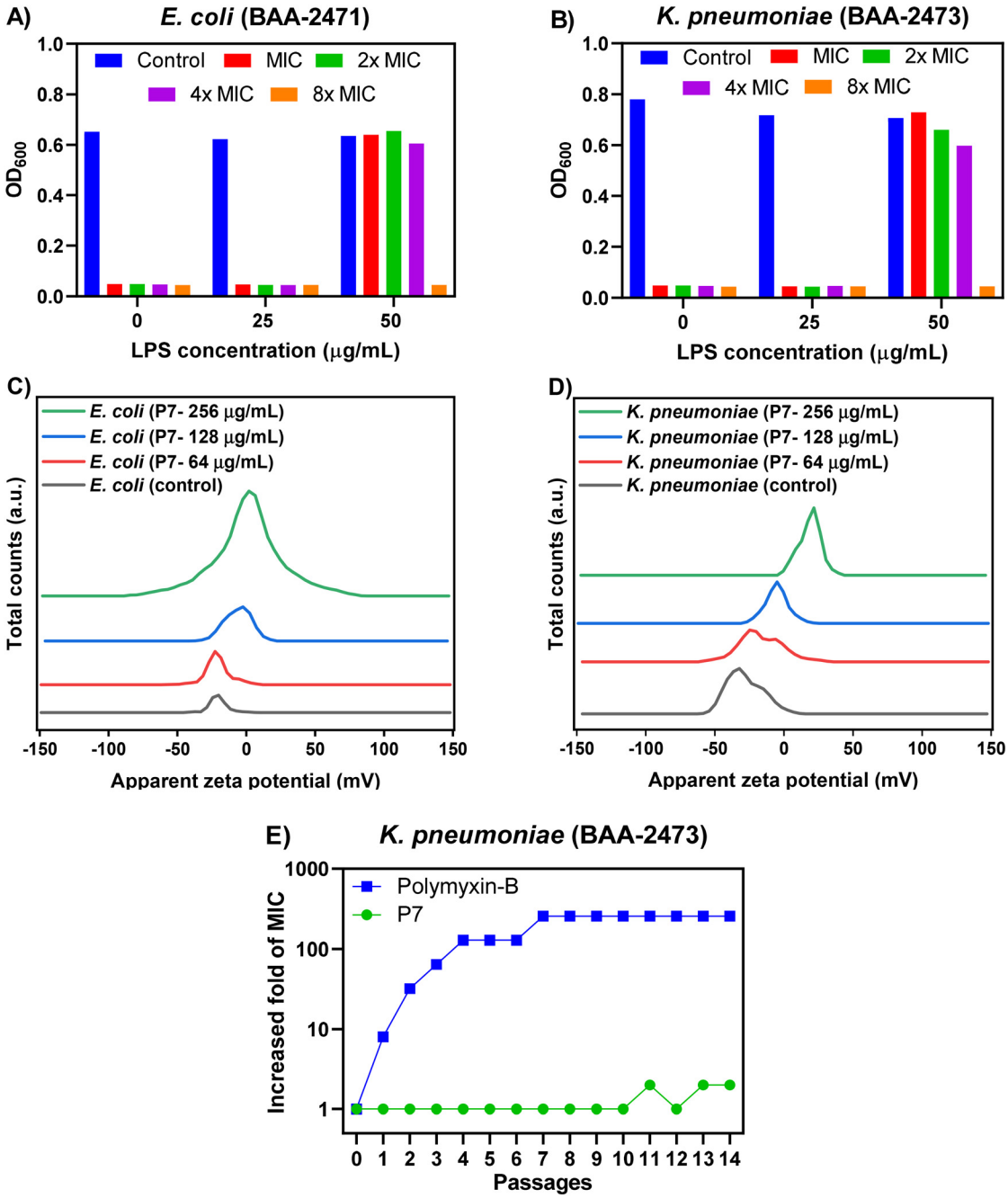

Fig. 4 LPS inhibition assay with the treatment of P7 (**PAEMA-dmCC**69%): (A) MDR *E. coli* (BAA-2471) and (B) MDR *K. pneumoniae* (BAA-2473); bacterial surface charge alteration with the treatment of P7 (**PAEMA-dmCC**69%): (C) MDR *E. coli* (BAA-2471) and (D) MDR *K. pneumoniae* (BAA-2473); (E) resistance development with the treatment of P7 (**PAEMA-dmCC**69%) and polymyxin-B: MDR *K. pneumoniae* (BAA-2473).

caused membrane depolarization showing the dose-dependent killing efficiency of MDR bacteria. Another crucial aspect of Gram-negative bacteria is the negatively charged LPS, an essential molecule integrated throughout the outer membrane. An increase in the MIC_{90} of copolymer P7 in the presence of LPS molecules revealed strong electrostatic interactions. This was further evidenced by observing the change in the surface charge of the bacterial solution from negative to positive zeta potentials with the addition of copolymer P7. Finally, the resistance profile of the copolymer was measured for a period of two weeks against MDR *K. Pneumoniae* (BAA-2473), which showed a minimal increase in the MIC_{90} for our copolymer treatment, whereas Polymyxin-B, a last-resort antibiotic, failed to inhibit resistance. These investigations revealed that cobaltocenium in combination with the primary ammonium-containing methacrylate polymer yields an effective antimicrobial

AMP mimicking metallopolymer and to our knowledge this is the first cobaltocenium copolymer that can act as a standalone therapeutic agent without the use of antibiotics.

4. Conclusions

In summary, we synthesized a new library of copolymers by incorporating two distinct cationic species to maintain amphiphilic balance. The inclusion of cobaltocenium endowed the polymers with broad-spectrum antimicrobial activity and enabled rapid eradication of NDM-1 producing bacteria without altering the overall cationic charge density. Mechanistic investigations revealed membrane-targeting properties *via* outer membrane permeabilization and membrane depolarization. The copolymers' high selectivity and low propensity to resistance can be ascribed to their membrane-perturbing mechanism and strong electrostatic interaction with LPS molecules, also demonstrated *via* bacterial surface charge alteration. Notably, the lead polymer was immune to bacterial resistance development. These findings establish metallopolymers with tunable amphiphilicity as promising therapeutic candidates to combat the escalating antibiotic crisis while unveiling a new frontier in AMP-mimicking polymer design.

5. Experimental section

5.1. Materials

All reagents were purchased from commercial sources and used as received unless stated otherwise. 2-Aminoethyl methacrylate hydrochloride (AEMA·HCl) was purchased from Aaron Chemicals. 2-Cyano-2-propyl benzodithioate (CPB) was purchased from Boron Molecular. *N*-(3-Dimethylaminopropyl)-*N*′-ethylcarbodiimide hydrochloride (EDC·HCl) was purchased from Oakwood Chemicals. Sulfo-NHS (*N*-hydroxysulfosuccinimide sodium salt 97%) was purchased from Ambeed, Inc. 2,2′-Azobis(2-methylpropionitrile) (AIBN, Sigma-Aldrich, 98%) and solvents such as dimethylformamide (DMF), dimethyl sulfoxide (DMSO), and dichloromethane (DCM) were purified by standard procedures. Deionized water was purified using a Millipore water purification system with a minimum resistivity of 18.2 megaohms per cm.

5.2. Polymer synthesis and characterization

5.2.1 Synthesis of poly(2-aminoethyl methacrylate) (PAEMA). 2-Aminoethyl methacrylate (AEMA) was polymerized by using the Reversible Addition–Fragmentation Chain Transfer (RAFT) polymerization technique. A typical protocol was as follows. In a 25 mL Schlenk flask the monomer AEMA (1 g, 6.04 mmol) was first dissolved in anhydrous DMF (1.5 mL) before adding AIBN (1.5 mg, 0.009 mmol) and CPB (10.03 mg, 0.045 mmol). A stock solution of both AIBN and CPB was prepared for all polymerizations. After three freeze–pump–thaw cycles, the flask was filled with nitrogen. The flask was immersed in a preheated oil-bath set at 70 °C and kept for a certain amount of time for achieving the desired molecular weight. The reaction mixture was quenched by cooling it in an ice bath and exposing it to air. The polymer solution was precipitated out in excess DCM and the solid polymer was collected. After drying, it was redissolved in DMF and precipitated at least 3 times. Later, the viscous polymer was dried under vacuum to obtain the polymer. The obtained **PAEMA** polymer was confirmed by ^{1}H NMR. The ^{1}H NMR spectrum of **PAEMA** is presented in (Fig. S1†). ^{1}H NMR (400 MHz, D_2O): δ = 0.90–1.20 (3H, –CH_2-C-C$\boldsymbol{H_3}$), δ = 1.94–2.30 (2H, –C$\boldsymbol{H_2}$-C-CH_3), δ = 3.36–3.52 (2H, –CH_2-C$\boldsymbol{H_2}$-NH_2·HCl), δ = 4.20–4.50 (2H, –O-C$\boldsymbol{H_2}$-CH_2), δ = 7.48–8.05 (5H, phenyl).

5.2.2 Synthesis of cobaltocenium- and dimethyl substituted cobaltocenium-containing PAEMA (PAEMA-CC and PAEMA-dmCC). Cobaltocenium carboxylic acid and dimethyl substituted cobaltocenium carboxylic acid were synthesized according to the previously reported literature.[57] Using approximately 50% cobaltocenium-containing polymer synthesis as an example, P3 (**PAEMA-CC**50%) was obtained using a typical amidation protocol as follows: cobaltocenium carboxylic acid (137.1 mg, 0.362 mmol) and sulfo-NHS (78.67 mg, 0.362 mmol) were dissolved in 3 mL of DMSO in a 25 mL round bottom flask. EDC·HCl (289.4 mg, 1.51 mmol) was dissolved in 1 mL of DMSO and added dropwise at 0 °C in the reaction flask. The mixture was stirred at 30 °C for not more than 1 h. **PAEMA** (50 mg, 0.302 mmol) was dissolved in 2 mL of water and added to the reaction mixture. The reaction was stirred at 30 °C for 2 days. Diethyl ether was used to wash the mixture repeatedly. After vacuum drying the crude mixture, it was dissolved in DI water. Then dialysis was performed with a cellulose ester membrane with MWCO 0.5–1 kDa for 2 days. For ion exchange from PF_6^- to Cl^-, the polymer solution was stirred with excess sodium chloride for several hours and again subjected to dialysis for over 1 day. The polymer solution was freeze-dried to get the final product. The final product was characterized by ^{1}H NMR. The ^{1}H NMR of **P2** is presented in Fig. S2.† ^{1}H NMR (400 MHz, D_2O): δ = 0.60–1.20 (3H, –CH_2-C-C$\boldsymbol{H_3}$), δ = 1.62–2.30 (2H, –C$\boldsymbol{H_2}$-C-CH_3), δ = 3.28–3.52 (2H, –CH_2-C$\boldsymbol{H_2}$-NH_2·HCl), δ = 3.58–3.85 (2H, –CH_2-C$\boldsymbol{H_2}$-NH–(C═O)–), δ = 3.96–4.50 (2H, –O-C$\boldsymbol{H_2}$-CH_2-NH_2–), δ = 5.8–5.97 (5H, *Cp*), δ = 5.97–6.10 (2H, *Cp*), δ = 6.25–6.46 (2H, *Cp*). The ^{1}H NMR of **P3** is presented in Fig. S3.† ^{1}H NMR (400 MHz, D_2O): δ = 0.50–1.30 (3H, –CH_2-C-C$\boldsymbol{H_3}$), δ = 1.50–2.26 (2H, –C$\boldsymbol{H_2}$-C-CH_3), δ = 3.22–3.43 (2H, –CH_2-C$\boldsymbol{H_2}$-NH_2·HCl), δ = 3.50–3.75 (2H, –CH_2-C$\boldsymbol{H_2}$-NH–(C═O)–), δ = 3.85–4.36 (2H, –O-C$\boldsymbol{H_2}$-CH_2-NH_2–), δ = 5.75–5.86 (5H, *Cp*), δ = 5.86–5.97 (2H, *Cp*), δ = 6.15–6.32 (2H, *Cp*). The ^{1}H NMR of **P4** is presented in Fig. S4.† ^{1}H NMR (400 MHz, D_2O): δ = 0.36–1.1 (3H, –CH_2-C-C$\boldsymbol{H_3}$), δ = 1.38–2.18 (2H, –C$\boldsymbol{H_2}$-C-CH_3), δ = 3.16–3.34 (2H, –CH_2-C$\boldsymbol{H_2}$-NH_2·HCl), δ = 3.39–3.70 (2H, –CH_2-C$\boldsymbol{H_2}$-NH–(C═O)–), δ = 3.74–4.22 (2H, –O-C$\boldsymbol{H_2}$-CH_2-NH_2–), δ = 5.67–5.80 (5H, *Cp*), δ = 5.80–5.93 (2H, *Cp*), δ = 6.08–6.27 (2H, *Cp*).

For the dimethyl substituted cobaltocenium-containing polymer, a similar protocol was used. The ^{1}H NMR of **P5** is presented in Fig. S6.† ^{1}H NMR (400 MHz, D_2O): δ = 0.60–1.36 (3H, –CH_2-C-C$\boldsymbol{H_3}$), δ = 1.57–2.50 (2H, –C$\boldsymbol{H_2}$-C-CH_3), δ = 1.99–2.17 (3H, *Cp*-C$\boldsymbol{H_3}$), δ = 2.27–2.47 (3H, *Cp*-C$\boldsymbol{H_3}$), δ = 3.25–3.45 (2H,

–CH_2-C***H***$_2$-NH_2·HCl), δ = 3.45–3.91 (2H, –CH_2-C***H***$_2$-NH–(C═O)–), δ = 3.94–4.38 (2H, –O-C***H***$_2$-CH_2-NH_2–), δ = 5.55–5.86 (7H, *Cp*), δ = 5.96–6.18 (2H, *Cp*). The ^{1}H NMR of **P6** is presented in Fig. S7.† ^{1}H NMR (400 MHz, D_2O): δ = 0.58–1.40 (3H, –CH_2-C-C***H***$_3$), δ = 1.55–2.60 (2H, –C***H***$_2$-C-CH_3), δ = 1.99–2.16 (3H, *Cp*-C***H***$_3$), δ = 2.26–2.46 (3H, *Cp*-C***H***$_3$), δ = 3.00–3.38 (2H, –CH_2-C***H***$_2$-NH_2·HCl), δ = 3.43–3.92 (2H, –CH_2-C***H***$_2$-NH–(C═O)–), δ = 3.93–4.41 (2H, –O-C***H***$_2$-CH_2-NH_2–), δ = 5.51–5.87 (7H, *Cp*), δ = 5.97–6.20 (2H, *Cp*). The ^{1}H NMR of **P7** is presented in Fig. S8.† ^{1}H NMR (400 MHz, D_2O): δ = 0.50–1.30 (3H, –CH_2-C-C***H***$_3$), δ = 1.53–2.46 (2H, –C***H***$_2$-C-CH_3), δ = 1.93–2.12 (3H, *Cp*-C***H***$_3$), δ = 2.22–2.40 (3H, *Cp*-C***H***$_3$), δ = 3.00–3.38 (2H, –CH_2-C***H***$_2$-NH_2·HCl), δ = 3.38–3.89 (2H, –CH_2-C***H***$_2$-NH–(C═O)–), δ = 3.89–4.41 (2H, –O-C***H***$_2$-CH_2-NH_2–), δ = 5.48–5.90 (7H, *Cp*), δ = 5.92–6.20 (2H, *Cp*).

5.2.3 Polymer size and zeta potential measurements by dynamic light scattering (DLS). A Zetasizer Nanoseries ZEN3690 (Malvern Instruments, Malvern, UK) instrument was used to measure the hydrodynamic diameter (D_H) and zeta potential of the copolymers. The samples were prepared by dissolving copolymers in filtered deionized water with varying concentrations (all solutions were filtered with a 0.22 μm PTFE membrane filter). The measurements were carried out at 25 °C and taken in triplicate at each concentration. The data processing was done using the general-purpose algorithms provided in Zetasizer software. Sample measurements were acquired in triplicate and reported as an average.[59]

5.3. Measurement of antibacterial activity

Escherichia coli (ATCC-11775), *Pseudomonas aeruginosa* (ATCC-10145), *Enterobacter cloacae* (ATCC-13047), *Acinetobacter baumannii* (ATCC-19606), MRSA-1 (BAA-1717), MRSA-2 (BAA-44), MDR *E. coli*-1 (BAA-2452), MDR *E. coli*-2 (BAA-2471), MDR *E. hormaechei* (BAA-2468), MDR *K. pneumoniae* (BAA-2473), and MDR *P. aeruginosa* (BAA-2108) were purchased from ATCC. Bacteria were streaked on tryptic soy agar (TSA) plates from their primary glycerol stock. After incubation at 37 °C for 24 h, a single colony was inoculated in 3 mL of tryptic soy broth (TSB) at 37 °C for 6 h under constant shaking at 190 rpm to reach the mid-log phase. Specific antibiotics were used in both TSA plates and TSB for specific bacteria: imipenem (25 μg mL^{-1}) for MDR *E. coli*-2 (BAA-2471), MDR *E. cloacae* (BAA-2468), and MDR *K. pneumoniae* (BAA-2473). All bacteria were adjusted to an optical density of 0.5 McFarland standard (OD_{600} = 0.70) for further use.

5.3.1 Minimum inhibitory concentration (MIC) assay. The MIC assay was performed according to the reported protocol.[61] Different concentrations of polymers in 50 μL of M9 solution using a 2-fold dilution method were added to 96-well plates. Then, 50 μL of bacteria containing M9 solution (~10^5 CFU per mL) was transferred to each well. Bacterial solutions and media without compounds were used as the positive control, and only media with compounds were used as the negative control. The prepared 96-well plate was placed in an incubator at 37 °C and shook at 190 rpm for 16–18 h. The bacterial growth was measured by reading OD_{600} values using a SpectraMax M5 Multimode Microplate Reader, Molecular Devices. The MIC_{90} was determined as the lowest concentration of the compound that completely inhibited at least 90% of bacterial growth. Each test was performed three times, with triplicate measurements for accuracy.

5.3.2 Hemolytic activity. All experimental procedures were approved by the University of South Carolina Institutional Animal Care and Use Committee (IACUC) under AUP# 2508, following the guidelines of the National Research Council for the Care and Use of Laboratory Animals. Blood was collected from mice in heparinized tubes and washed with PBS containing 10% FBS. Polymers were prepared in PBS at varying concentrations and added to the blood in a 96-well plate (150 μL per well). PBS with 0.2% Triton X-100 served as the maximal lysis control. The samples were incubated at 37 °C for 1 hour, and then centrifuged at 400*g* for 10 minutes. Following centrifugation, 100 μL of supernatant from each well was transferred to a new 96-well plate, and absorbance was measured at 450 nm. PBS with 10% FBS was used for background readings. The hemolysis was calculated as:

$$\frac{\text{Sample OD} - \text{background}}{\text{Max lysis OD} - \text{background}}$$

5.3.3 Time-kill kinetics against planktonic phase bacteria. The kinetic killing assay was performed similarly as described in the MIC assay. MDR *E. coli* and MDR *K. pneumoniae* bacteria were treated with P4, P6, and P7. Mid-log phase (~10^8 CFU per mL) bacterial cell cultures were suspended to ~10^5 CFU per mL in media. 50 μL of bacteria containing media was mixed with 50 μL of polymer solutions in media of MIC and higher concentrations. The plate was incubated at 37 °C for 24 h. As a negative control, 50 μL of sterile water was used instead of any compounds. At 0 h, 2 h, 4 h, 8 h, and 12 h, 20 μL of media from each concentration was then 10-fold serially diluted in normal saline (0.9% NaCl). From these dilutions, 20 μL aliquots were spot plated onto tryptic agar plates and incubated at 37 °C for 24 hours. After incubation, viable colonies were counted. The detection limit of this experiment was 80 CFU per mL. All experiments were conducted in duplicate.

5.3.4 Time-kill kinetics against stationary phase bacteria. Stationary-phase bacteria were prepared as follows: a mid-log phase bacterial culture (~10^8 CFU per mL) was diluted to 1 : 1000 in nutrient broth (NB) and incubated at 37 °C with shaking at 190 rpm for 16 hours. Following incubation, the culture was centrifuged at 3500*g* for 5 minutes, and the supernatant was removed. The bacterial pellet was resuspended in normal saline. The stationary cells were then used for kinetic experiments, following the same procedure as time-kill kinetics against planktonic bacterial cells. All experiments were performed in duplicate. Bacteria were treated with P4 and P7, while water was used as a negative control.

5.3.5 Outer membrane permeabilization assay. Bacterial cultures were grown in TSB broth and incubated overnight at 37 °C in a shaking incubator. A 10 μL aliquot of the overnight culture was diluted in 10 mL of fresh NB broth until the optical density (OD) reached 0.2–0.6. The bacterial culture was

then centrifuged at 3500*g* for 5 minutes, and the supernatant was removed. The pellet was resuspended in 1× PBS and subsequently suspended in a 1 : 1 mixture of 5 mM HEPES and 5 mM glucose buffer. *N*-Phenyl naphthylamine (NPN) dye was added to the bacterial suspension at a final concentration of 10 μM. A Corning black and clear bottom 96-well plate was prepared, with 180 μL of the prepared bacterial suspension added to each well. The fluorescence intensity of the NPN dye was measured at an excitation wavelength of 350 nm and an emission wavelength of 420 nm every 2 minutes. After 4 minutes, 20 μL of the test compound in water was added to the wells, with the final concentration adjusted using the microdilution method. The fluorescence intensity was recorded for an additional 24 minutes. Wells containing 20 μL of water instead of the compound served as negative controls. All experiments were performed in triplicate.[60]

5.3.6 Membrane depolarization assay. Bacterial cultures were grown in TSB broth and incubated for 6 h at 37 °C in a shaking incubator to reach the mid-log phase. A 10 μL aliquot of the culture was diluted into 10 mL of fresh NB broth and further incubated at 37 °C until the optical density (OD) reached 0.2–0.6. The bacterial culture was then centrifuged at 3500*g* for 5 minutes, and the supernatant was removed. The bacterial pellet was resuspended in 1× PBS and subsequently suspended in a 1 : 1 : 1 mixture of 5 mM HEPES buffer, 5 mM glucose, and 100 mM KCl solution and 0.2 mM ethylenediaminetetraacetic acid (EDTA) was added additionally for Gram-negative bacteria. $DiSC_3$ (3,3′-dipropylthiadicarbocyanine iodide) was added to the bacterial suspension to a final concentration of 2 μM, and the mixture was incubated in darkness for 1 hour. A Corning black and clear bottom 96-well plate was prepared with 180 μL of the bacterial suspension per well. The fluorescence intensity of the $DiSC_3$ dye was measured at an excitation wavelength of 622 nm and an emission wavelength of 670 nm every 2 minutes. After 4 minutes, 20 μL of the test compound in Millipore water was added, with the final concentration adjusted using the microdilution method. The fluorescence intensity was recorded for an additional 24 minutes. Wells containing 20 μL of Millipore water instead of the compound served as negative controls. All experiments were performed in triplicate.[44]

5.3.7 LPS inhibition assay. The LPS inhibition assay was performed for P7 against MDR *E. coli* and MDR *K. pneumoniae* by a slight modification of a previously reported method.[49] In a 96-well plate, 100 μL of P7 (256 μg mL^{-1} in M9) was added in the first well, and then 50 μL was taken from the first well and was serially diluted to the sixth well. 50 μL of LPS (25 μg mL^{-1} in M9) was added to each well. After that, 100 μL of bacteria containing media was added to each well. The plate was incubated at 37 °C overnight and the optical density (OD) was measured. This was repeated for 50 μg mL^{-1} LPS. The positive and negative controls were, respectively, LPS and P7 incubated in the media. Each measurement was taken in triplicate.

5.3.8 Bacterial surface charge alteration. Bacteria cultures were grown in the TSB broth and incubated for 6 h at 37 °C to reach the mid-log phase. The bacterial culture was then centrifuged at 3500*g* for 5 minutes, and the supernatant was removed. The bacterial pellet was resuspended in 1× PBS for washing. After removing PBS, the bacterial pellet was resuspended in M9 media. 1 mL of bacteria containing media was transferred to a sterile dry quartz cuvette and the zeta potential was measured using a Zetasizer Nano. The measurement was taken in triplicate. Then polymer was added to the bacterial solution to adjust the polymer concentration to 64 μg mL^{-1} and the zeta potential was measured in triplicate. The same was followed to measure the zeta potential at polymer concentrations of 128 μg mL^{-1} and 256 μg mL^{-1} in media in the presence of bacteria.

5.3.9 Resistance study. The resistance development study was conducted following a previously reported protocol.[17] The experiment was performed for P7 (**PAEMA-dmCC**69%) against MDR *K. pneumoniae*, with Polymyxin-B included for comparison as a last-resort antibiotic for Gram-negative infections. MIC values were first determined using standard procedures. For subsequent passages, bacterial cultures were prepared from those exposed to sub-MIC ($\frac{1}{2}$ MIC) concentrations of the compound. This process was repeated for 14 consecutive passages. Resistance development was assessed by calculating fold changes in the MIC relative to the initial MIC and plotted over the passage number. All experiments were performed in triplicate.

Author contributions

M. W. H: writing – original draft, investigation, formal analysis, and methodology; I. B: writing – review & editing, formal analysis, and methodology; S. B: writing – review & editing, formal analysis, and methodology; A. A: formal analysis; A. P: formal analysis; X. Y: formal analysis and methodology; P. N: writing – review & editing; M. N: writing – review & editing; C. T: writing – original draft, conceptualization, supervision, investigation, formal analysis, resources, and funding acquisition. All authors approved the final version of the manuscript.

Conflicts of interest

There are no conflicts to declare.

Data availability

The data supporting this article have been included as part of the ESI.†

Acknowledgements

The authors acknowledge the University of South Carolina for financial support. The partial funding support from the National Institutes of Health (R01AI149810) is also acknowl-

edged. We would also like to acknowledge BioRender for the TOC image (created in BioRender by Hossain, M. W. (2025); https://BioRender.com/nax4lzk).

References

1 I. N. Okeke, M. E. A. de Kraker, T. P. Van Boeckel, C. K. Kumar, H. Schmitt, A. C. Gales, S. Bertagnolio, M. Sharland and R. Laxminarayan, *Lancet*, 2024, **403**, 2426–2438.
2 S. Barman, L. B. Kurnaz, R. Leighton, M. W. Hossain, A. W. Decho and C. Tang, *Biomaterials*, 2024, 122690.
3 K. Lewis, *Cell*, 2020, **181**, 29–45.
4 M. I. Hutchings, A. W. Truman and B. Wilkinson, *Curr. Opin. Microbiol.*, 2019, **51**, 72–80.
5 G. D. Wright, *Chem. Commun.*, 2011, **47**, 4055.
6 G. D. Wright, *Trends Microbiol.*, 2016, **24**, 862–871.
7 H. I. Zgurskaya, C. A. Lopez and S. Gnanakaran, *ACS Infect. Dis.*, 2015, **1**, 512–522.
8 *WHO bacterial priority pathogens list, 2024: bacterial pathogens of public health importance, to guide research, development, and strategies to prevent and control antimicrobial resistance*, World Health Organization, 2024.
9 L. Maryam, S. Khalid, A. Ali and A. U. Khan, *Future Microbiol.*, 2019, **14**, 671–689.
10 M. Shahid, N. Ahmad, N. K. Saeed, M. Shadab, R. M. Joji, A. Al-Mahmeed, K. M. Bindayna, K. S. Tabbara and F. K. Dar, *Front. Cell. Infect. Microbiol.*, 2022, **12**, 1033305.
11 P. Pham, S. Oliver and C. Boyer, *Macromol. Chem. Phys.*, 2023, **224**, 2200226.
12 M. Zasloff, *Nature*, 2002, **415**, 389–395.
13 Z. Song, Z. Han, S. Lv, C. Chen, L. Chen, L. Yin and J. Cheng, *Chem. Soc. Rev.*, 2017, **46**, 6570–6599.
14 M. Xiong, Z. Han, Z. Song, J. Yu, H. Ying, L. Yin and J. Cheng, *Angew. Chem., Int. Ed.*, 2017, **56**, 10826–10829.
15 A. A. Bahar and D. Ren, *Pharmaceuticals*, 2013, **6**, 1543–1575.
16 R. E. Hancock, M. A. Alford and E. F. Haney, *Nat. Rev. Microbiol.*, 2021, **19**, 786–797.
17 S. Barman, L. B. Kurnaz, X. Yang, M. Nagarkatti, P. Nagarkatti, A. W. Decho and C. Tang, *ACS Infect. Dis.*, 2023, **9**, 1769–1782.
18 Y. Chen, L. Yu, B. Zhang, W. Feng, M. Xu, L. Gao, N. Liu, Q. Wang, X. Huang, P. Li and W. Huang, *Biomacromolecules*, 2019, **20**, 2230–2240.
19 C. H. Chen and T. K. Lu, *Antibiotics*, 2020, **9**, 24.
20 G. N. Tew, R. W. Scott, M. L. Klein and W. F. Degrado, *Acc. Chem. Res.*, 2010, **43**, 30–39.
21 E. F. Palermo and K. Kuroda, *Appl. Microbiol. Biotechnol.*, 2010, **87**, 1605–1615.
22 T. Zhu, Y. Sha, J. Yan, P. Pageni, M. A. Rahman, Y. Yan and C. Tang, *Nat. Commun.*, 2018, **9**, 4329.
23 M. Zhou, Y. Qian, J. Xie, W. Zhang, W. Jiang, X. Xiao, S. Chen, C. Dai, Z. Cong, Z. Ji, N. Shao, L. Liu, Y. Wu and R. Liu, *Angew. Chem., Int. Ed.*, 2020, **59**, 6412–6419.
24 H. Takahashi, G. A. Caputo and K. Kuroda, *Biomater. Sci.*, 2021, **9**, 2758–2767.
25 K. Kuroda and W. F. Degrado, *J. Am. Chem. Soc.*, 2005, **127**, 4128–4129.
26 M. F. Ilker, K. Nüsslein, G. N. Tew and E. B. Coughlin, *J. Am. Chem. Soc.*, 2004, **126**, 15870–15875.
27 K. Lienkamp, K. N. Kumar, A. Som, K. Nüsslein and G. N. Tew, *Chem. – Eur. J.*, 2009, **15**, 11710–11714.
28 E. F. Palermo and K. Kuroda, *Biomacromolecules*, 2009, **10**, 1416–1428.
29 E. H. Wong, M. M. Khin, V. Ravikumar, Z. Si, S. A. Rice and M. B. Chan-Park, *Biomacromolecules*, 2016, **17**, 1170–1178.
30 P. R. Judzewitsch, T. K. Nguyen, S. Shanmugam, E. H. H. Wong and C. Boyer, *Angew. Chem., Int. Ed.*, 2018, **57**, 4559–4564.
31 P. R. Judzewitsch, L. Zhao, E. H. H. Wong and C. Boyer, *Macromolecules*, 2019, **52**, 3975–3986.
32 J. Xie, M. Zhou, Y. Qian, Z. Cong, S. Chen, W. Zhang, W. Jiang, C. Dai, N. Shao, Z. Ji, J. Zou, X. Xiao, L. Liu, M. Chen, J. Li and R. Liu, *Nat. Commun.*, 2021, **12**, 5898.
33 A. Vishwakarma, F. Dang, A. Ferrell, H. A. Barton and A. Joy, *J. Am. Chem. Soc.*, 2021, **143**, 9440–9449.
34 J. Yan, X. Zhang, P. Xu, J. Zhang, X. Li, F. Zhong, Y. Xu, Q. Zhang, Y. Zhu and Y. Yan, *Adv. Mater. Technol.*, 2025, **10**, 2401559.
35 G. R. Whittell, M. D. Hager, U. S. Schubert and I. Manners, *Nat. Mater.*, 2011, **10**, 176–188.
36 C. G. Hardy, L. Ren, J. Zhang and C. Tang, *Isr. J. Chem.*, 2012, **52**, 230–245.
37 L. Zhao, X. Liu, L. Zhang, G. Qiu, D. Astruc and H. Gu, *Coord. Chem. Rev.*, 2017, **337**, 34–79.
38 Y. Wang, D. Astruc and A. S. Abd-El-Aziz, *Chem. Soc. Rev.*, 2019, **48**, 558–636.
39 M. R. Roner, C. E. Carraher Jr, K. Shahi and G. Barot, *Materials*, 2011, **4**, 991–1012.
40 M. Patra, G. Gasser and N. Metzler-Nolte, *Dalton Trans.*, 2012, **41**, 6350–6358.
41 G. Gasser and N. Metzler-Nolte, *Curr. Opin. Chem. Biol.*, 2012, **16**, 84–91.
42 F. Li, J. G. Collins and F. R. Keene, *Chem. Soc. Rev.*, 2015, **44**, 2529–2542.
43 A. S. Abd-El-Aziz, C. Agatemor and N. Etkin, *Biomaterials*, 2017, **118**, 27–50.
44 J. Hwang, S. Barman, R. Gao, X. Yang, A. O'Malley, P. Nagarkatti, M. Nagarkatti, M. Chruszcz and C. Tang, *Adv. Healthcare Mater.*, 2023, **12**, e2301764.
45 J. Zhang, Y. P. Chen, K. P. Miller, M. S. Ganewatta, M. Bam, Y. Yan, M. Nagarkatti, A. W. Decho and C. Tang, *J. Am. Chem. Soc.*, 2014, **136**, 4873–4876.
46 P. Yang, M. Bam, P. Pageni, T. Zhu, Y. P. Chen, M. Nagarkatti, A. W. Decho and C. Tang, *ACS Infect. Dis.*, 2017, **3**, 845–853.
47 Z. Si, W. Zheng, D. Prananty, J. Li, C. H. Koh, E. T. Kang, K. Pethe and M. B. Chan-Park, *Chem. Sci.*, 2022, **13**, 345–364.

48 S. Hong, H. Takahashi, E. T. Nadres, H. Mortazavian, G. A. Caputo, J. G. Younger and K. Kuroda, *PLoS One*, 2017, **12**, e0169262.
49 Q. Zhou, K. Li, K. Wang, W. Hong, J. Chen, J. Chai, L. Yu, Z. Si and P. Li, *Sci. Adv.*, 2024, **10**, eadp6604.
50 R. Namivandi-Zangeneh, Z. Sadrearhami, D. Dutta, M. Willcox, E. H. H. Wong and C. Boyer, *ACS Infect. Dis.*, 2019, **5**, 1357–1365.
51 S. C. Williams, M. B. Chosy, C. K. Jons, C. Dong, A. N. Prossnitz, X. Liu, H. L. Hernandez, L. Cegelski and E. A. Appel, *ACS Cent. Sci.*, 2025, **11**, 486–496.
52 J. Zhang, Y. Yan, M. W. Chance, J. Chen, J. Hayat, S. Ma and C. Tang, *Angew. Chem., Int. Ed.*, 2013, **52**, 13387–13391.
53 S. Wickramasinghe, A. Hoehn, S. T. Wetthasinghe, H. Lin, Q. Wang, J. Jakowski, V. Rassolov, C. Tang and S. Garashchuk, *J. Phys. Chem. B*, 2023, **127**, 10129–10141.
54 T. Zhu, Y. Sha, H. A. Firouzjaie, X. Peng, Y. Cha, D. M. M. M. Dissanayake, M. D. Smith, A. K. Vannucci, W. E. Mustain and C. Tang, *J. Am. Chem. Soc.*, 2020, **142**, 1083–1089.
55 H. Lin, L. Ramos, J. Hwang, T. Zhu, M. W. Hossain, Q. Wang, S. Garashchuk and C. Tang, *Macromolecules*, 2023, **56**, 6375–6384.
56 L. He, E. S. Read, S. P. Armes and D. J. Adams, *Macromolecules*, 2007, **40**, 4429–4438.
57 L. Ren, C. G. Hardy, S. Tang, D. B. Doxie, N. Hamidi and C. Tang, *Macromolecules*, 2010, **43**, 9304–9310.
58 Y. Lou, J. Gaitor, M. Treichel, K. J. T. Noonan and E. F. Palermo, *ACS Macro Lett.*, 2023, **12**, 215–220.
59 M. A. Rahman, Y. Cha, L. Yuan, P. Pageni, T. Zhu, M. S. Jui and C. Tang, *J. Polym. Sci.*, 2020, **58**, 77–83.
60 L. B. Kurnaz, S. Barman, X. Yang, C. Fisher, F. W. Outten, P. Nagarkatti, M. Nagarkatti and C. Tang, *Biomaterials*, 2023, **301**, 122275.
61 A. H. Delcour, *Biochim. Biophys. Acta, Proteins Proteomics*, 2009, **1794**, 808–816.
62 M. A. Farha, C. P. Verschoor, D. Bowdish and E. D. Brown, *Chem. Biol.*, 2013, **20**, 1168–1178.